2019

Using a comparative approach to investigate the relationship between landscape and genetic connectivity among woodland salamander population

Alexander C. Camercon
University of New Mexico

Robert B. Page
Texas A&M University

James I. Watling
John Carroll University, jwatling@jcu.edu

Cari-Ann M. Hickerson
John Carroll University, chickerson@jcu.edu

Carl Anthony
John Carroll University, canthony@jcu.edu

Follow this and additional works at: https://collected.jcu.edu/fac_bib_2019

Part of the Biology Commons, and the Genetics Commons

Using a comparative approach to investigate the relationship between landscape and genetic connectivity among woodland salamander population

Alexander C. Cameron· Robert B. Page · James I. Watling · Cari-Ann M. Hickerson · Carl D. Anthony

Abstract

For many amphibian species, reduced landscape connectivity results in reduced genetic connectivity among populations. However, large effective population sizes (N_e) slow the rate of genetic drift, causing subdivided populations to remain genetically similar despite little gene flow among them. Therefore, it is important to address the combined effects of N_e and matrix permeability to quantify the relative importance of gene flow and genetic drift on isolated amphibian populations. We applied a landscape genetic approach to investigate how patterns of gene flow (m), N_e (inferred via θ) and genetic differ-entiation differ among Eastern Red-backed Salamander (*Plethodon cinereus*) populations in a fragmented landscape ($n = 4$) compared to a continuous forest ($n = 4$). We assayed a panel of 10 microsatellite markers for population genetic analyses. Additionally, we constructed and validated a distribution model to generate resistance surfaces for examining the relation-ship between landscape connectivity, m, θ, and genetic differentiation (F_{ST}) using maximum-likelihood population-effects models (MLPE). Populations in continuous habitat were undifferentiated, whereas fragmented populations exhibited genetic structure driven by a single population. Results of the MLPE models in the fragmented landscape revealed spatial variation in θ as the best predictor of pairwise F_{ST}, followed by estimates of m, suggesting migration-drift interactions have a stronger influence on genetic differentiation than matrix permeability. Moreover, model coefficients for landscape resistance were comparable between landscapes. Overall, our results provide insight as to how the interaction of gene flow and genetic drift shapes population structure for a dispersal-limited species within a predominately anthropogenic landscape.

Keywords Fragmentation · Gene flow · Genetic drift · Maximum-likelihood population-effects models · Microsatellites · Red-backed salamander · Species distribution models

Introduction

Dispersal and gene flow patterns among populations are often influenced by landscape connectivity, the degree to which landscape features either facilitate or impede the movement of organisms (Spear et al. 2010). Habitat loss and fragmentation often lead to reduced landscape con-nectivity and altered dispersal patterns for organisms that inhabit modified environments (Hanski 1998). Moreover, the genetic consequences of reduced or altered gene flow associated with habitat fragmentation (e.g. decreased genetic diversity and increased inbreeding) weakens the viability of metapopulations and increases the probability of regional extinction (Templeton et al. 2001; Cushman et al. 2016). Numerous studies have demonstrated that decreased land-scape connectivity in fragmented landscapes leads to a reduction in genetic connectivity, threatening the persistence

and adaptive potential of populations across a variety of taxa (Vandergast et al. 2007; Fenderson et al. 2014; Barr et al. 2015).

Habitat loss and fragmentation are known to be major contributors in the global decline of amphibians (Almedia-Gomes and Rocha 2014). Amphibians are generally characterized by low vagility and frequently exhibit site fidelity (Duellman and Trueb 1986). Therefore, it is usually assumed that amphibians have poor dispersal capabilities and often exist as metapopulations (Alford and Richards 1999; but see Marsh and Trenham 2001), relying on periodic long-distance dispersal events to maintain gene flow among populations (Semlitsch 2008). Poor dispersal capacity and pronounced metapopulation structure are factors that often magnify the genetic consequences of habitat fragmentation experienced by amphibians (Gibbs 1998a; Bowne and Bowers 2004). Woodland salamanders (genus *Plethodon*), like most amphibians, are characterized as dispersal limited (Liebgold et al. 2011). Dispersal limitation is likely linked to the physiological constraints imposed by being lungless, especially for fully terrestrial species. Terrestrial plethodontids occupy moist habitats to maintain cutaneous respiration, constraining the extent to which they can move due to desiccation risk (Watling and Braga 2015). Additionally, the small body size of *Plethodon* salamanders likely contributes to dispersal limitation, as maximum dispersal distance and vagility exhibit a positive relationship with body mass among amphibians (Hillman et al. 2014).

The Eastern Red-backed Salamander, *Plethodon cinereus*, (red-backed salamander hereafter) is an abundant, terrestrial woodland species distributed throughout Eastern North America, and has long served as a focus of study in behavioral and community ecology (Jaeger and Forester 1993; Mathis et al. 1995; Anthony and Pfingsten 2013; Jaeger et al. 2016). Additionally, there is a growing interest in understanding the population dynamics of red-backed salamanders from a genetic perspective. Surveys of neutral genetic variation (i.e. microsatellites) for this species have addressed a variety of topics including: identifying barriers to gene flow (Marsh et al. 2007, 2008), divergence among color morphs (Fisher-Reid et al. 2013; Grant and Liebgold 2017; Hantak et al. 2019), and philopatry (Liebgold et al. 2011). As such, red-backed salamanders have been considered an indicator species for other woodland salamander species, and more broadly forest ecosystem function and integrity (Welsh and Droege 2001; Davic and Welsh 2004).

Although several studies have investigated how landscape connectivity affects genetic variation among red-backed salamander populations, the relationship remains unclear, and may be complicated by historical genetic signatures of post-glacial range expansion (Cabe et al. 2007; Noël et al. 2007; Jordan et al. 2009; Noël and Lapointe 2010). For example, within unaltered or continuous landscapes,

southern populations of red-backed salamanders exhibit weak, but detectable differentiation at distances as close as 200 m (Virginia: Cabe et al. 2007), whereas northerly populations in formerly glaciated areas are genetically homogeneous at distances up to 4.1 km (Quebec: Noël et al. 2007). Furthermore, molecular surveys conducted in altered landscapes present a varied genetic response to the effects of habitat fragmentation, particularly within formerly glaciated regions. Fragmented populations of red-backed salamanders have been characterized as both strongly differentiated over small spatial scales (0.9–3.3 km, Quebec: Noël et al. 2007) and minimally differentiated across broad spatial scales (70 km, Indiana: Jordan et al. 2009; 35 km, Montréal: Noël and Lapointe 2010). One explanation for a lack of genetic differentiation among fragmented populations is that high local densities reduce genetic drift (Gibbs 1998b; Jordan et al. 2009). Therefore, genetic similarities among some fragmented populations may be attributed to weak genetic drift as opposed to high gene flow (see Jordan et al. 2009 for additional discussion). However, how gene flow and genetic drift interact to influence genetic variation among red-backed salamander populations in fragmented landscapes must be addressed.

Here we compare patterns of genetic diversity and differentiation among red-backed salamander populations in fragmented and continuous landscapes in the formerly glaciated regions of Ohio and Pennsylvania, USA. We compared gene flow in both landscape types to investigate whether genetic structuring among populations is a result of reduced dispersal in the fragmented landscape, evaluated the relationship between pairwise genetic distance and several landscape attributes, and used estimates related to effective population size (θ: $4N_e \mu$) to assess the relationship between the strength of genetic drift and patterns of genetic differentiation. We predicted that geographic distance would limit gene flow in both landscape types for dispersal-limited red-backed salamanders. However, we expected to see a greater influence of matrix resistance on genetic connectivity in the fragmented landscape because of reduced landscape permeability. Finally, if genetic differentiation in the fragmented landscape is driven by rapid genetic drift, we expected populations with higher N_e sizes to be less differentiated, given that the strength of genetic drift is inversely proportional to N_e.

Materials and methods

Locality description

The study area was divided into two landscape types, fragmented and continuous, with four focal sites located in each. The four sites in the fragmented landscape are located

in a heavily urbanized portion of Cuyahoga County, OH (Fig. 1a, c). These sites include: a cemetery (Lakeview Cemetery (LV); 114 ha; 41.510389°N–81.585018°W); a reclaimed golf course (Acacia Reservation (AR); 47 ha; 41.504196°N–81.494007°W); a reclaimed bluestone quarry (Euclid Creek (EC); 140 ha; 41.543354°N–81.527190°W); and an urban nature preserve (Doan Brook Valley (DB); 112 ha; 41.493723°N–81.593795°W). These site boundaries were designated in the late nineteenth century and are separated by distances ranging from 1.9 to 8.4 km (Fig. 1c). The continuous sites were located in the Allegheny National Forest, Forest and Warren Counties, Pennsylvania (Fig. 1a, b), which was established in the early twentieth century. The continuous habitat was located approximately 300 km

from the fragmented habitat and at similar latitude. The spatial arrangement of sites in the Allegheny National Forest mirrored those in the fragmented habitat to reduce the effect of geographic distance as a confounding variable for comparison of gene flow estimates (Minister Creek Site 1(MC1): 41.6244324°N–79.1599585°W; Minister Creek Site 2(MC2): 41.6395770°N–79.1579901°W; Minister Creek Site 3(MC3): 41.6715618°N–79.2225819°W; Minister Creek Site 4(MC4): 41.6122014°N–79.2239427°W). Distances between sites within the Allegheny National Forest range from 1.7 to 6.7 km (Fig. 1b). Finally, red-backed salamanders are polymorphic for dorsal color and recent studies have suggested that color morphs may differ in dispersal tendencies (Grant and Liebgold 2017) and in territory
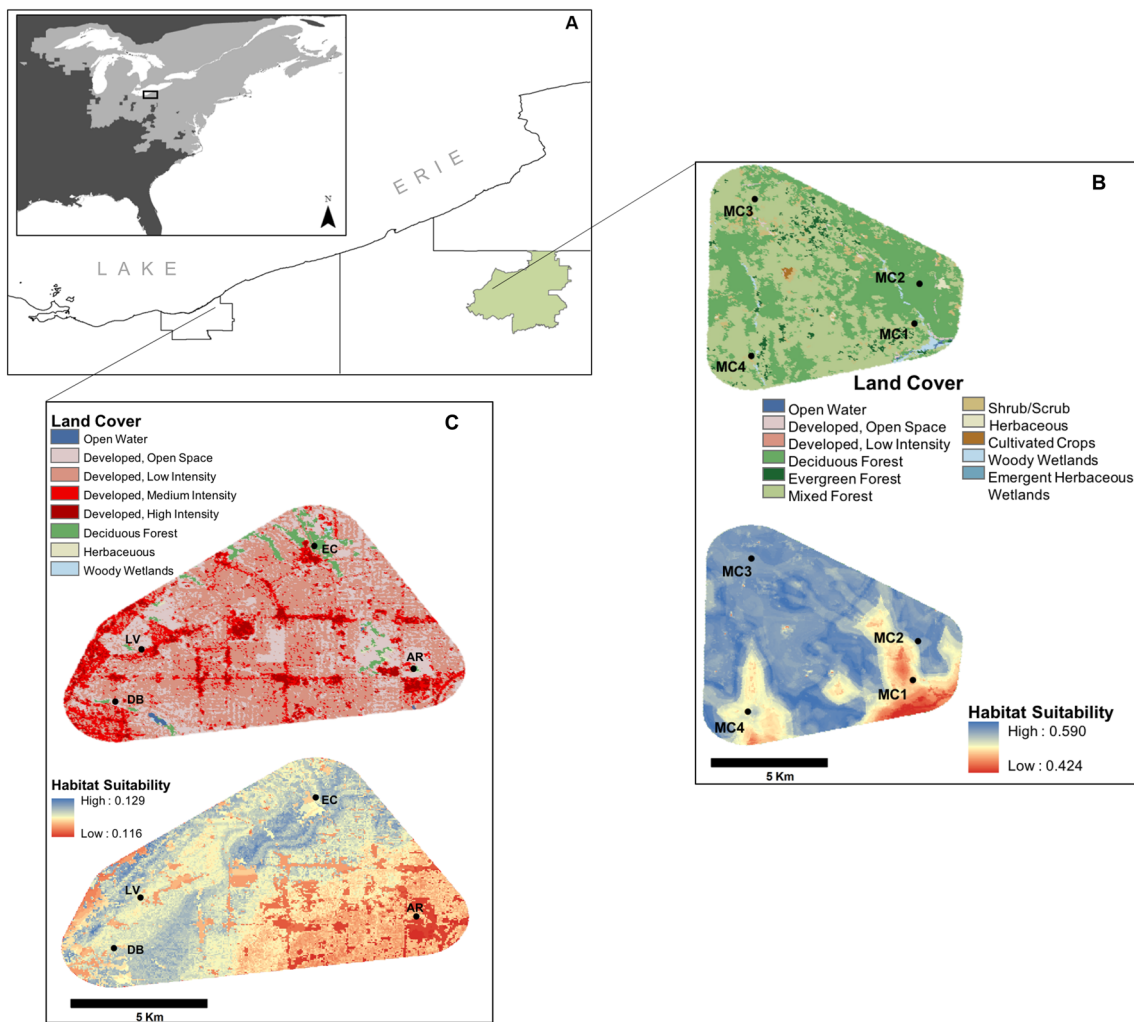

Fig. 1 Focal region, land use and predicted suitability of sampled areas. **a** Inset depicting the range of the Eastern Red-backed salamander and highlighted focal region. The fragmented landscape is located in Cuyahoga Co. Ohio (left) and the continuous landscape is located within the Allegheny National Forest in Pennsylvania (right). **b** Land use (top) and predicted suitability (bottom) for the continuous sample sites. Sites are shown within spatially constrained landscapes used to estimate resistance at a 30 m resolution. Distances between sites range from 1.7 to 6.7 km. **c** Land use (top) and predicted suitability maps (bottom) for the fragmented sample sites are shown within spatially constrained landscapes used to estimate resistance at a 30 m resolution. Distances between sites range from 1.9 to 8.4 km. (Color figure online)

fidelity (Reiter et al. 2014). Therefore, all of the sampled sites are monomorphic for the striped phenotype to eliminate color morph as a factor in dispersal.

DNA Isolation and PCR-based genotyping

We obtained 120 tail samples from each landscape type (30 individuals from each site) between 23 March and 5 May of 2015. Genomic DNA was extracted from tail tips using the Wizard Genomic DNA Purification Kit (Promega) following the manufacturer's instructions. We assayed ten microsatellite loci for red-backed salamanders described in Cameron et al. (2017; *Pc3*, *Pc7*, *Pc13*, *Pc14*, *Pc16*, *Pc17*, *Pc25*, *Pc28*, *Pc34*, *Pc37*).

All genotyping reactions followed a nested Polymerase Chain Reaction (PCR) protocol described by Schuelke (2000), with final volumes of 25 µl containing 10–100 ng DNA template, 1× buffer, 1.5 mM MgCl$_2$, 0.2 mM of each dNTP, 0.8 µM non-M13(-21)-twinned primer, 0.8 µM FAM labeled M13(-21) primer, 0.2 µM M13(-21)-twinned primer, and 0.625 units of GoTaq polymerase (Promega). Cycling conditions followed Cameron et al. (2017). Successful amplification was confirmed via electrophoresis using 2% agarose gels stained with ethidium bromide and fragment analysis was performed using an Applied Biosystems 3730 (Arizona State University) with GENESCAN 600 as the internal sizing standard. Geneious version 9.1.2 (Biomatters) was used to manually score, bin, and assign genotypes.

Quality control and summary statistics

The presence of null alleles, large allele dropout, and scoring errors was examined using MICRO-CHECKER version 2.2.3 (Van Oosterhout et al. 2004). We estimated observed (H$_O$) and expected (H$_E$) heterozygosity to test for significant departures from Hardy–Weinberg proportions using GENEPOP version 4.3 (Rousset 2008). Additionally, GENEPOP was used to test for genotypic disequilibrium and to compute the Weir and Cockerham (1984) estimator of F$_{IS}$. Finally, GENEALEX version 6.5 (Peakall and Smouse 2012) and *PopGenKit* (Paquette 2012) were used to calculate statistics characterizing genetic diversity, including the number of alleles per locus, number of effective alleles, number of private alleles, and allelic richness.

Genetic differentiation and population structure

The degree of genetic differentiation among sites within each landscape was measured using two G-statistics. Global and pairwise comparisons of G$_{ST}$ values were calculated based on Nei and Chesser's (1983) unbiased estimators of H$_S$ (i.e. the Hardy–Weinberg expected heterozygosity averaged across all populations) and H$_T$ (i.e. the Hardy–Weinberg expected heterozygosity in the total population ignoring subdivision), where G$_{ST}$ = (H$_T$ − H$_S$)/H$_T$. Additionally, we calculated global and pairwise comparisons of G″$_{ST}$, which is formulated to equal one when populations have non-overlapping allele sets, irrespective of the level of genetic diversity (Meirmans and Hendrick 2011). Both G-statistics were calculated in GENEALEX and all associated *P* values are based on 9999 permutations.

We used STRUCTURE 2.3.4 (Pritchard et al. 2000) to estimate the number of genetic clusters present within each landscape type. Ten independent runs of STRUCTURE were performed for each landscape, each with a randomly generated seed, testing values of *K* = 1 to *K* = 5. Each Markov Chain Monte Carlo (MCMC) run consisted of 350,000 iterations that were discarded as burn-in with an additional 350,000 iterations for sampling. When appropriate, we repeated this procedure within the genetic clusters identified by STRUCTURE to detect population substructure. STRUCTURE HARVESTER web version 0.6.94 (Earl and von-Holdt 2012) was used to calculate Δ*K* (Evanno et al. 2005) and CLUMPP version 1.1.2 (Jakobosson and Rosenberg 2007) was used to align the replicate runs of the Δ*K* with highest likelihood. We then performed an analysis of molecular variance (AMOVA; Excoffier et al. 1992) in GENEALEX to investigate the hierarchical partitioning of genetic variation (1) among STRUCTURE clusters (2) among individuals within STRUCTURE clusters, and (3) within individuals. Given that the AMOVA was performed on the clustering results from STRUCTURE, we do not report the associated *P* values due to issues of non-independence (Meirmans 2015). Additionally, we visualized the ordination of individuals in genetic space without imposing model constraints via Discriminant Analysis of Principle Components (DAPC: Jombart et al. 2010). We used K-means clustering to obtain clustering solutions for K = 1–10, and the Bayesian information criterion (BIC) to evaluate which value of K to use as prior cluster assignments in the DAPC. The optimal number of principal components to retain was determined prior to DAPC analysis via cross-validation (Jombart and Collins 2015).

Estimating gene flow

Although results from the coalescent based software MIGRATE (Beerli 2008, 2009) have traditionally been interpreted as reflecting historical rates of gene flow, evidence from recent simulations suggests MIGRATE produces gene flow estimates that better reflect contemporary gene flow patterns (Samarasin et al. 2017). Therefore, we implemented the Bayesian option of MIGRATE v 3.6.11 to estimate migration (*m*: proportion of immigrants) and effective population size (*θ*: 4N$_e$ µ) and interpreted *m* as estimates of contemporary gene flow. A Brownian motion model was used to approximate a step-wise mutation model, with relative mutation

rates for each locus estimated from the data. We used slice sampling for four replicate long chains for 25,000,000 iterations sampling every 500 iterations and discarded the first 5,000,000 iterations as burn-in. Estimates of m and θ were modeled with a uniform prior with lower and upper boundaries of 0 and 3000 for m and 0 and 100 for θ with F_{ST} values used for initial estimates of both m and θ. Output was assessed by visual inspection of posterior distributions and the effective sample sizes for parameter estimates (ESS). Values of the estimated parameters were considered accurate if the ESS was ≥ 1000 (Converse et al. 2015). The estimated values of m and θ were scaled by a standard microsatellite mutation rate of 5×10^{-4} (Garza and Williamson 2001) as this general mutation has been shown to be similar to approximated mutation rates (Yue et al. 2007; Converse et al. 2015).

Population bottlenecks and effective population size

We tested for evidence of recent population bottlenecks in both landscapes using three different methods. First, we examined deviations from expected heterozygosity at drift-mutation equilibrium using the program BOTTLENECK (Piry et al. 1999). Deviations were assessed under the stepwise mutation model (SMM), infinite alleles model (IAM) and the two-phase mutation model (TPM). Under the TPM, we assumed 95% of all mutations were single-step mutations with 12% of the variance within multistep mutations (Piry et al. 1999). We ran 1000 iterations, and used the Wilcoxon signed-rank test implemented in BOTTLENECK to determine whether deviations were significant. The program BOTTLENECK was also used to implement a Mode-shift test that assesses whether there has been a shift in allele frequency distributions. Finally, M-ratios were calculated using the output from GENEALEX and were assessed against the recommended critical value of 0.68 (Garza and Williamson 2001). Effective population size (N_e) estimates were generated via the linkage disequilibrium (Waples and Do 2008) and the heterozygote-excess (Zhdanova and Pudovkin 2008) methods implemented in NeESTIMATOR (Do et al. 2014).

Landscape genetic analyses

We constructed a resistance surface to estimate connectivity among populations in each landscape. Resistance surface values were derived from habitat suitability predictions from an ensemble distribution model constructed with the BIOMOD package implemented in R (Thuiller et al. 2009; R Core Team 2016). The ensemble model represents a consensus prediction of habitat suitability based on the unweighted averages from two different modeling algorithms (Random Forest, Breiman 2001; Generalized Boosted Models, Friedman 2002). We modeled habitat suitability for the entire geographic range of the red-backed salamander using the following variables: annual mean temperature, mean temperature of wettest and driest quarter, annual precipitation and precipitation of wettest and driest quarter, www.worldclim.org; elevation, www.usgs.gov; percent canopy cover (Hansen et al. 2013); and land cover (Homer et al. 2015). All environmental predictor variables were resampled to a resolution of 30 m in ArcGIS v.10.3. Presence data consisted of geo-referenced accounts of *P. cinereus* collected between 1990 and 2015 obtained from VertNet (www.VertNet.org) and the Global Biodiversity Information Facility (www.GBIF.org). Observations from each database were combined, and duplicate observations removed. In an attempt to exclude potentially erroneous observations, occurrence points that fell outside a 10 km buffer of the documented geographic range of *P. cinereus* (www.iucnredlist.org) were removed. The final data set consisted of 1,188 unique presence observations spanning the species' geographic range.

Five replicate models were run for each algorithm, with 75% of the occurrence data randomly partitioned for model training and the remaining 25% partitioned for model testing. Model performance was evaluated using three traditional cross-validation metrics as well as specificity and sensitivity metrics. In addition to traditional model validation metrics, we also assessed the relationship between habitat suitability and salamander counts in the continuous landscape. Testing the relationship between model predictions and salamander counts in both landscapes would have been ideal; however, the location of the fragmented landscape within a highly populated area imposed logistical constraints and resulted in a non-random sampling of the environment. We surveyed 59 randomly-generated and spatially independent observations within the Allegheny National Forest. Each observation represents a 5×5 m plot that was systematically surveyed by four researchers. All 59 plots were sampled over the course of four sampling events between 26 September and 8 November 2016 (Fig. 2a). We used zero-inflated models to relate species counts to suitability. The results of fitting salamander count data to predicted suitability revealed a strong, positive relationship between salamander density and suitability, indicating the ensemble model was able to detect a biological response to changes in landscape quality ($z = 3.605$; $P < 0.001$; Fig. 2b). Landscape resistance was calculated by subtracting predicted suitability from 1 (Fig. 1b, c). For greater detail regarding model construction, validation, and the relationship between model predictions and salamander counts, see the supplemental methods and results. (Online Resource 1).

The resistance layer was used to estimate connectivity using electrical circuit theory in CIRCUITSCAPE (McRae et al. 2008). However, CIRCUITSCAPE does not impose constraints on how much of the landscape an organism uses; therefore, the more landscape that is included, the higher the probability that resistance values may include biologically
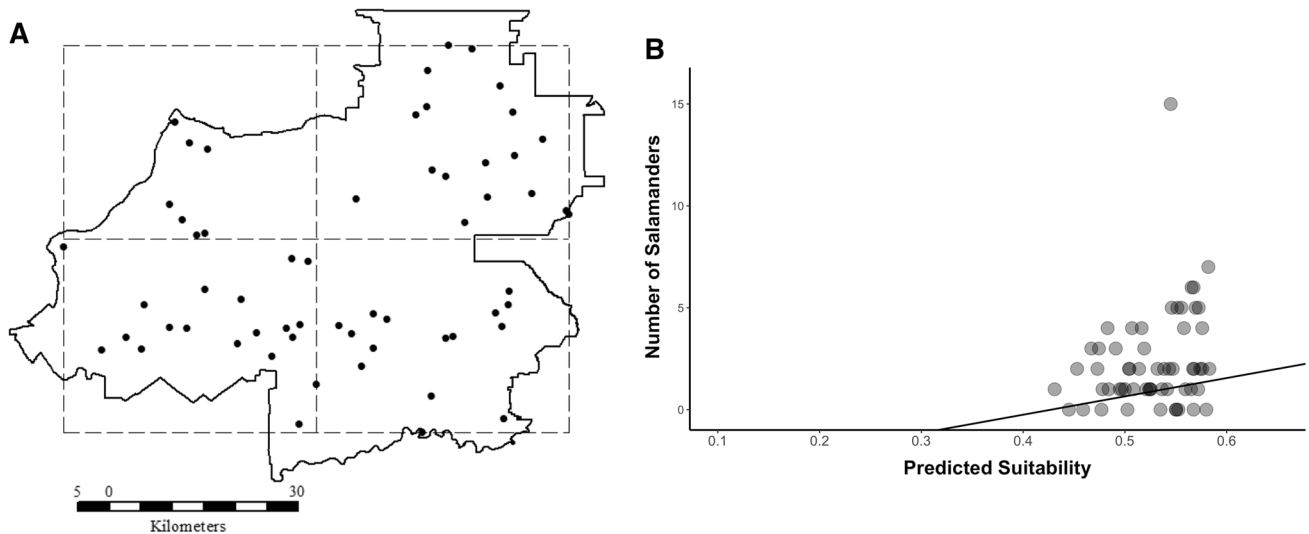
Fig. 2 Relating predicted suitability to salamander counts. **a** Map illustrating how the ANF was divided into four quadrants for sampling independent species observations. Each point represents a 5 × 5 m plot that was systematically surveyed for red-backed salamanders. **b** Relationship between red-back salamander counts and predicted suitability estimates from the ensemble SDM. After cor-

recting for zero-inflation there was a highly significant relationship between salamander count data and model predictions ($z = 3.605$; $P < 0.001$). Ensemble model predictions indicate that for every one-unit change in suitability, salamander counts should increase by nearly 9 individuals ($y = 8.98x + - 3.849$)

unrealistic dispersal pathways among populations. To reduce extraneous connections within each landscape, a minimum convex polygon encompassing the four sites was created, and buffered by 1.44 km (Fig. 1b, c). The spatially constrained resistance layers were used as the input for the calculation of pairwise effective resistance matrices for both landscape types by CIRCUITSCAPE.

For both landscapes, we populated pairwise matrices with effective resistance, geographic (straight line) distance, and linearized F_{ST} values (Slatkin 1995). Additionally, we used the estimates of m and theta produced by MIGRATE to infer the importance of gene flow and genetic drift in determining patterns of genetic differentiation. For both parameters, we populated pairwise matrices with the mean value between sites. Larger values of m between sites should correspond to less differentiation as a result of gene flow and larger values of theta between sites should correspond to less drift induced differentiation. Geographic distance was log transformed prior to analysis to better approximate normality, and all predictor variables were centered and scaled to allow for the comparison of model coefficients. We tested for correlation among predictor variables by performing Mantel tests (Mantel 1967) within the *ade4* package (Dray and Dufour 2007). Correlated ($r \geq 0.65$) predictor variables were excluded from appearing in the same model.

To evaluate the relationship between predictor variables and pairwise F_{ST}, we used maximum-likelihood population-effects (MLPE) models, as this method explicitly addresses the dependency of pairwise observations (Clarke et al. 2002).

We initially fit MLPE models using maximum likelihood for parameter estimation to allow for model selection using AIC_C via the *MuMIn* package in R (Bartoń 2013). The top candidate models identified in each landscape were then re-fit using REML for more precise parameter estimates. All MLPE models were fit using the functions provided in the *ResistanceGA* package (Peterman 2018). In addition to using an information theoretic criterion to assess model fit, we also estimated two marginal R^2 variants for models fit with REML. Both variants of R^2 describe the variance explained by the fixed effects. The first statistic estimated was R_β^2, which is derived from the methods of Edwards et al. (2008) and is implemented in the *r2glmm* package (Jaeger 2016). The second statistic was the marginal $R_{GLMM'm}^2$ following Nakagawa and Schielzeth (2013), which was implemented in the *MuMIn* package. Finally, we assessed the significance of model coefficients by calculating 95% confidence intervals using the *conint.merMod* function implemented in the *lme4* package (Bates et al. 2015), where significant predictors were identified by confidence intervals that did not overlap zero.

Results

Quality control and summary statistics

Two loci (*Pc13* and *Pc14*) were monomorphic in six out of eight populations and were subsequently removed from the

molecular data set prior to downstream analyses. Holm's (1979) correction for multiple testing was performed by treating the tests associated with each site as a family of tests. After correction, there were two statistically significant deviations from HWE, AR at *Pc25* and MC1 at *Pc7*. Deviations of *Pc25* and *Pc7* from HWE were at the population level and not the locus level; therefore, we opted to include the two loci in the final data set. MICRO-CHECKER detected evidence for null alleles at *Pc7* (MC1), *Pc16* (AR), *Pc17* (AR; MC2), *Pc25* (AR; EC; LV), *Pc28* (LV), and Pc37 (MC3). There was no statistical evidence of genotypic disequilibrium among any pairs of loci in either landscape after applying Holm's correction. Across all ten loci, 68 alleles were present in the fragmented landscape, while 48 alleles were present in the continuous landscape. Sites within the fragmented landscape tended to have slightly higher heterozygosity ($H_O = 0.366$–0.509; $H_E = 0.378$–0.596; Online Resource 2) compared to the continuous landscape ($H_O = 0.303$–0.341; $H_E = 0.319$–0.359; Online Resource 2). In addition, sites in the fragmented landscape tended to have higher allelic richness and a greater number of effective alleles compared to sites in the continuous landscape (Online Resource 2).

Genetic differentiation and population structure

Locus-specific estimates of G_{ST} in the fragmented landscape ranged from 0.025 to 0.263, and were all highly statistically significant after applying Holm's correction (maximum $P = 0.009$). The degree of differentiation observed for locus-specific G_{ST} estimates in the continuous landscape ranged from -0.008 to 0.029, with no loci exhibiting statically significant differentiation after correcting for multiple tests (minimum $P = 0.015$). The global G_{ST} value across eight loci was 0.116 ($P = 0.001$; $SE = 0.02$) in the fragmented landscape and 0.005 ($P = 0.056$; $SE = 0.004$) in the continuous landscape. Locus-specific estimates of G''_{ST} for the fragmented landscape ranged from 0.057 to 0.712, and were also statistically significant (maximum $P = 0.011$). Similar to the results observed for estimates of G_{ST}, the locus-specific estimates of G''_{ST} for continuous landscape ranged from -0.015 to 0.059, and were not significantly different from zero after correcting for multiple tests. The global estimate of G''_{ST} across eight loci in the fragmented landscape was 0.382 ($P = 0.001$; $SE = 0.058$) while the global G''_{ST} in continuous landscape was 0.012 ($P = 0.056$; $SE = 0.010$). Pairwise comparisons of G_{ST} and G''_{ST} estimates within the fragmented landscape revealed marked differentiation between AR and the remaining sites (Table 1). We compared locus-specific estimates of G''_{ST} across landscape types using a paired *t* test and found there to be significantly more differentiation in the fragmented landscape compared to the continuous landscape ($t = 5.39$; $df = 7$; $P = 0.001$). However, calculating

locus-specific estimates of G''_{ST} in the fragmented landscape excluding AR revealed no statistical difference in the amount of genetic differentiation between landscapes ($t = 1.38$; $df = 7$ $P = 0.2902$).

The results of the STRUCTURE analysis for the fragmented sites revealed an optimal solution of $\Delta K = 2$, with little admixture between the two discrete genetic groupings (Fig. 3a; Online Resource 3). Further analysis of the cluster that consisted of EC, LV and DB revealed an optimal solution of $K = 1$, however we also visualized $K = 2$. (Fig. 3b; Online Resource 3). The optimal solution in the continuous landscape was also $\Delta K = 2$ (Fig. 3c; Online Resource 3). No alternative solutions for ΔK were explored for the continuous landscape, as $\Delta K = 2$ was over an order of magnitude greater than all other explored values of K.

Results of the AMOVA for the fragmented sites were consistent with the presence of moderate genetic structuring, with 15% of the genetic variation was apportioned to differences among clusters (Table 2). Presumably the variation attributed to differences among clusters is largely driven by the genetic dissimilarity of AR compared to the remaining sites, as indicated by the STRUCTURE results (Fig. 3a). Most genetic variation was attributed to differences within individuals. The AMOVA results for the continuous sites revealed the absence of population structuring, with only 1% of the genetic variation being partitioned to differences among clusters, 10% among individuals within clusters, and 89% of variation partitioned to differences within individuals (Table 2).

For the DAPC analyses performed on both landscape types, all discriminant functions were retained and the cross-validation procedure determined that 10 principal components was the optimal value to retain for both analyses. Within the fragmented landscape, K-means clustering and BIC indicated that K = 4–6 are essentially equally valid solutions (Online Resource 4.). We selected K = 4, as we determined this solution contained the most interpretable, and biologically relevant groupings. The DB and LV sites constituted the majority of 2 clusters (DB/LVcluster1: 11 DB, 15 LV, 3 EC, and 2 AR individuals; DV/LVcluster2: 14 DB, 9 LV, 2 EC, and 1 AR individual). While most EC individuals were assigned to a single cluster, individuals from DB and LV were also present in this cluster (EC cluster: 25 EC, 5 DB, 6 LV, and 1 AR individual). The last cluster was comprised of the 26 remaining individuals from the AR locality. Scatter plots of the first two discriminant functions shows the first discriminant function separates AR while the second discriminant function distinguishes the DB/LV clusters from the EC cluster (Fig. 4a). Within the continuous landscape, K-means and BIC evaluation determined K = 5 to be the optimal solution (Fig. 4b; Online Resource 4). However, each cluster contains nearly equal numbers of individuals from each site with the exception of "Cluster

Table 1 Pairwise comparisons of G_{ST} and G''_{ST} estimates across eight polymorphic loci for both the fragmented populations and continuous populations

Statistic: G_{ST}				
Fragmented	AR	DB	LV	EC
AR	*	0.102	0.101	0.127
DB	0.001	*	0.010	0.038
LV	0.001	0.009	*	0.019
EC	0.001	0.001	0.001	*
Statistic: G_{ST}				
Continuous	MC1	MC2	MC3	MC4
MC1	*	− 0.0002	0.006	0.015
MC2	0.481	*	− 0.002	0.003
MC3	0.068	0.753	*	− 0.001
MC4	0.003	0.185	0.529	*
Statistic: G''_{ST}				
Fragmented	AR	DB	LV	EC
AR	*	0.506	0.472	0.538
DB	0.001	*	0.042	0.148
LV	0.001	0.009	*	0.075
EC	0.001	0.001	0.001	*
Statistic: G''_{ST}				
Continuous	MC1	MC2	MC3	MC4
MC1	*	− 0.001	0.020	0.051
MC2	0.481	*	− 0.009	0.010
MC3	0.068	0.753	*	− 0.002
MC4	0.003	0.184	0.529	*

G_{ST} and G''_{ST} values are above the diagonal and corresponding *P* values below

3" which is comprised of five individuals from MC1 and two individuals from MC2 ("Cluster 1" = 7 MC1, 5 MC2, 6 MC3, 6 MC4 individuals; "Cluster 2" = 6 MC1, 9 MC2, 7 MC3, 5 MC4 individuals; "Cluster 4 = 9 MC1, 8 MC2, 10 MC3, 5 MC4 individuals; "Cluster 5" = 3 MC1, 6 MC2, 7 MC3, 14 MC4 individuals). In viewing the scatter plot of the first two discriminant functions, the first discriminant function parses out "Cluster 5" and "Cluster 3" while the second discriminate function aids in separating the remaining three clusters (Fig. 4b).

Estimating gene flow

For both landscapes, the posterior distributions over all loci for all parameter estimates were unimodally distributed and ESS values > 1000. Estimates of gene flow revealed similarly low levels of migration among sites in both landscapes (Fig. 5a; Fig. 5b). In the fragmented landscape, values of *m* ranged from 0.0037 to 0.0155 (Fig. 5a) which is similar to the majority of estimates

for the continuous landscape (Fig. 5b). The lowest values of *m* in the fragmented landscape corresponded to immigration into AR from the remaining sites (Fig. 5a). Across both landscapes, the proportion of immigrants did not exceed 1.5% with the exception of estimates of gene flow in the continuous landscape from MC2 into MC4 ($m = 0.139$; Fig. 5b). Theta estimates ranged from 16.7 (AR) to 179.2 (DB; Fig. 5a) in the fragmented landscape while estimates in the continuous landscape ranged from 616.7 (MC3) to 2172.2 (MC2; Fig. 5b).

Population bottlenecks and effective population size

Heterozygosity excess tests and *M*-ratios revealed little in the way of statistical evidence for population bottlenecks (Online Resource 5). Results from the Wilcoxon signed-rank test detected significant heterozygosity excess at two sites in each landscape (AR and LV in the fragmented landscape,
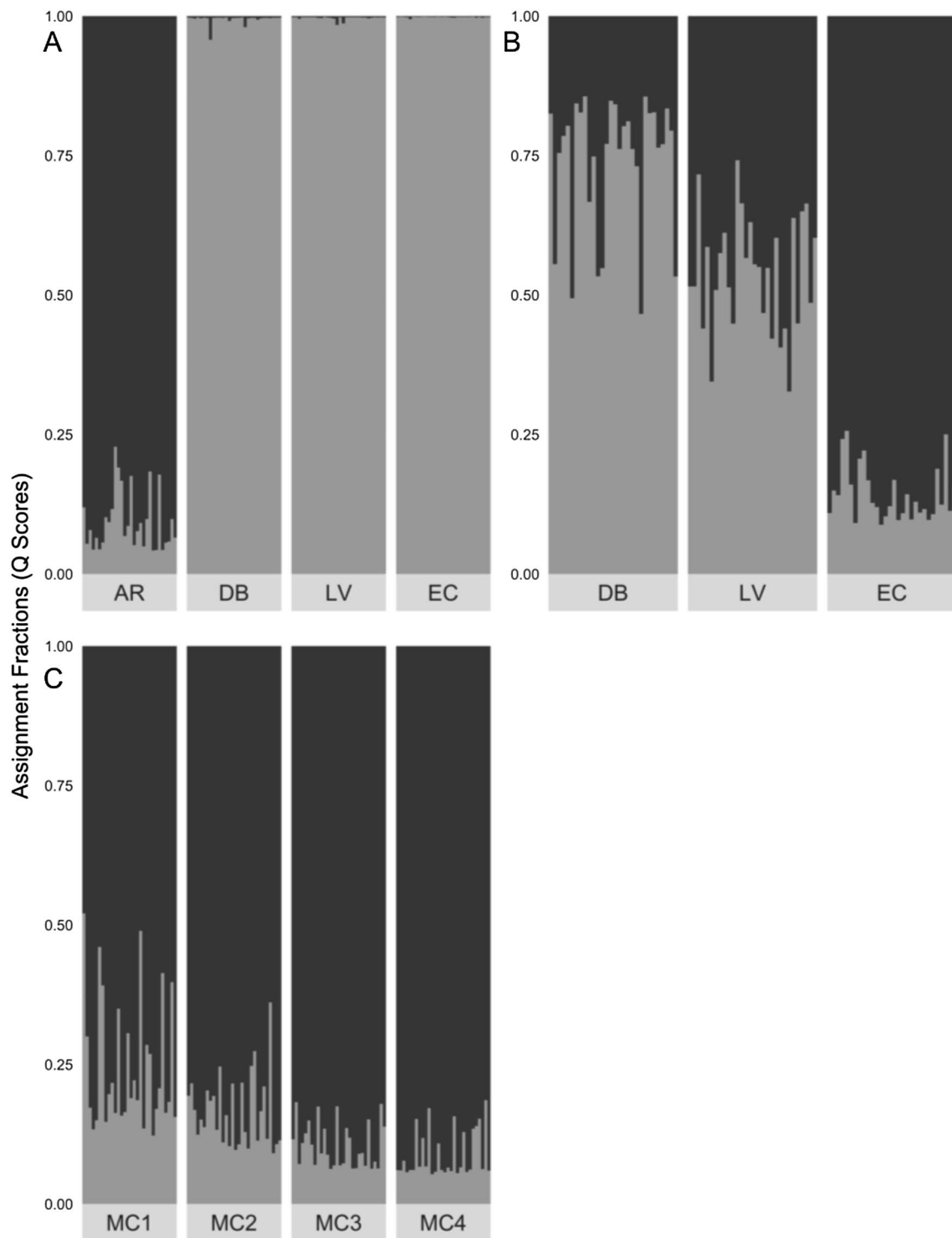
Fig. 3 Results from STRUCTURE analyses. **a** Population structure of red-backed salamanders within the fragmented landscape where $\Delta K = 2$. **b** Visualization of $K = 2$ for the cluster comprised of DB, LV, and EC however the optimal solution was $K = 1$. **c** Population structure of red-backed salamanders from continuous habitat where $\Delta K = 2$

and MC1 and MC3 in the continuous landscape), although results were not consistent across all three mutation models. Additionally, the Mode-shift test revealed that none of the sites exhibited a distorted allele frequency distribution, as would be expected following a bottleneck. Finally, none of the calculated M-ratios were below the critical value of 0.68,

Table 2 AMOVA results for both fragmented and continuous landscapes

| Landscape type	Source of variation	Degrees of freedom	Sum of squares	Variance component	Fixation Index
Fragmented	Among populations	2	64.183	0.395	$F_{ST} = 0.149$
	Among individuals	117	290.675	0.223	$F_{IS} = 0.099$
	Within individuals	120	244.500	2.038	$F_{IT} = 0.233$
	Total	239	599.358	2.656	N/A
Continuous	Among populations	3	8.1	0.012	$F_{ST} = 0.007$
	Among individuals	116	226.3	0.175	$F_{IS} = 0.099$
	Within individuals	120	192	1.600	$F_{IT} = 0.105$
	Total	239	464.4	1.788	N/A
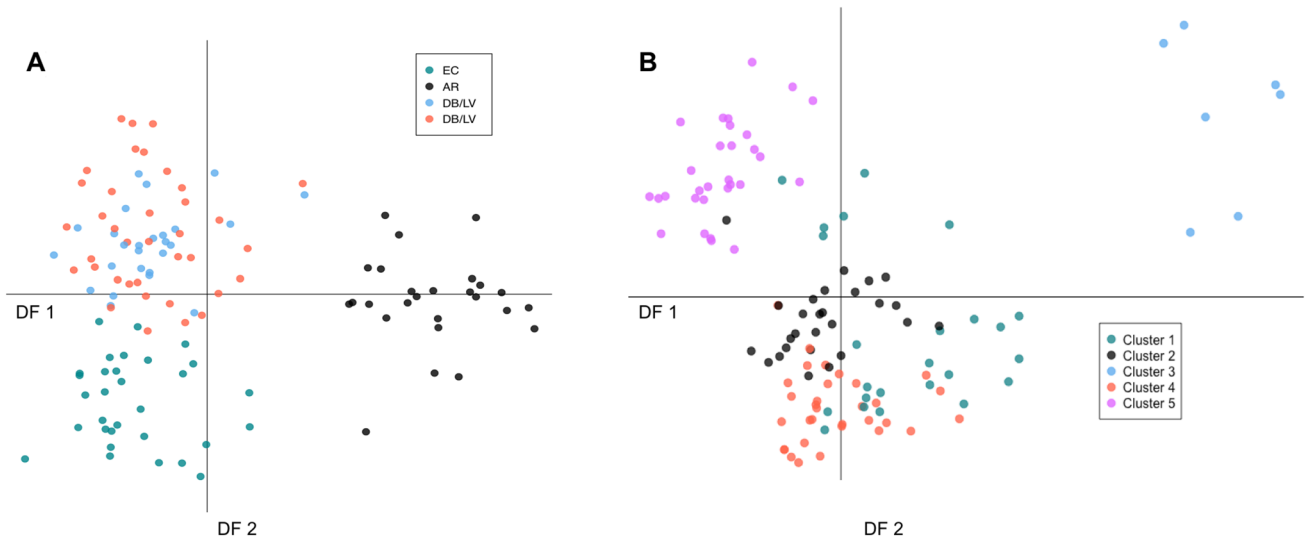
Fig. 4 DAPC scatter plots. **a** Scatter plot of the first two discriminant functions for the fragmented sites. Groupings were largely consistent with results from STRUCTURE. **b** Scatter plot of the first two discriminant functions for the continuous sites. K-means and BIC evaluation determined K = 5 to be the optimal solution, however, each cluster contains a nearly equal numbers of individuals from the original sites with the exception of "Cluster 3". (Color figure online)
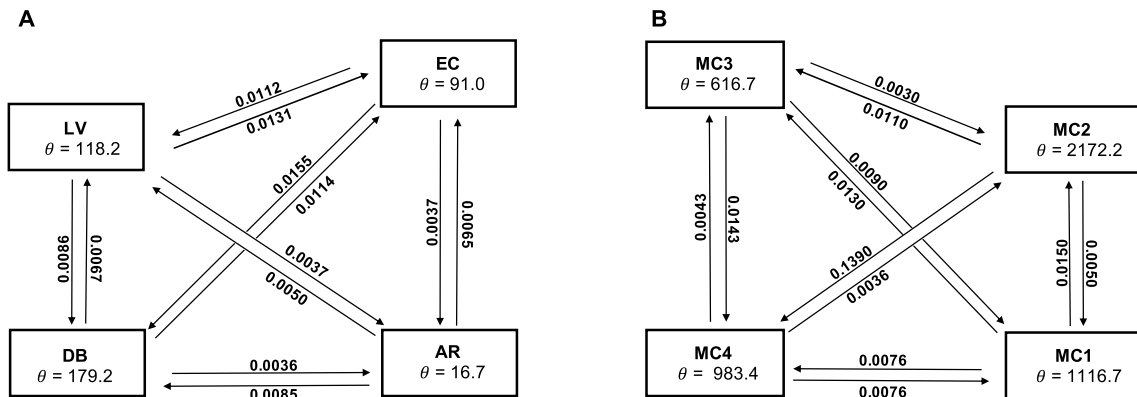

Fig. 5 Gene flow and theta estimates. **a** Gene flow estimates in the fragmented landscape where the proportion of immigrants is adjacent to the corresponding arrows. Within each rectangle are the estimates of theta. **b** Gene flow and theta estimates in the continuous landscape

although two sites in the fragmented landscape (EC, LV) and all four sites in the continuous landscape were within one SEM of the critical value (Online Resource 5).

NeESTIMATOR was unable to generate point estimates and/or confidence limits for N_e at all of the sites despite trying several minimum allele frequencies in addition to applying no frequency restriction. We focus on the information obtained via the linkage disequilibrium method with a minimum allele frequency set to equal 0.02, as the output from heterozygote-excess method was unable to calculate point estimates and confidence limits (i.e., all results were returned as "infinity"). We obtained point estimates for two sites in the fragmented landscape (DB = 120.6; LV = 108.8) and lower confidence limits for the remaining sites (EC = 41.8; AR = 165.9; Online Resource 6). Similarly, point estimates were recovered for two sites in the continuous landscape (MC1 = 82.8; MC4 = 265.5) and lower confidence limits for the remaining two sites (MC2 = 52.1; MC3 = 73; Online Resource 6).

Landscape genetic analyses

We investigated the association between landscape attributes, effective population size, gene flow, and genetic differentiation. In both landscapes, geographic distance and resistance were highly correlated, as were mean values of theta

and m. We did not detect a problematic degree of correlation among the remaining predictor variables. As such, we evaluated the fit of eight models in each landscape: $F_{ST} \sim$ Geo, $F_{ST} \sim$ Resist, $F_{ST} \sim$ Theta, $F_{ST} \sim m$, $F_{ST} \sim$ Geo + Theta, $F_{ST} \sim$ Resist + Theta, $F_{ST} \sim$ Geo + m, F_{ST} + Resist + m. The top four candidate models returned in each landscape following AIC_C model selection were all fit with single variables (Table 3).

Additionally, we calculated Cook's distance for the top model sets to determine if models in either landscape where overly influenced by a single observation (Cook 1977). All values returned were less than one and of a similar magnitude for all of the models considered. This is especially pertinent for the theta model in the fragmented landscape given the discrepancy in size of the estimates and indicates the larger means of theta among sites are equally as important as the smaller values in predicting F_{ST}.

In the fragmentated landscape, theta and m received significantly more support than did the models related to landscape attributes ($\Delta AIC_C > 2$). Moreover, theta and m were the only two variables to exhibit a significant relationship with pairwise F_{ST} (Table 3). While the ΔAIC_C was < 2 between theta and m, the R^2 statics revealed that theta accounted for substantial variation in pairwise F_{ST} ($R^2_\beta = 0.626$; $R^2_{GLMM'm} = 0.697$) compared to gene flow ($R^2_\beta = 0.048$; $R^2_{GLMM'm} = 0.035$) while resistance and geo-

Table 3 Maximum-likelihood population-effects model results investigating geographic distance (Geo), effective resistance (Resist), effective population size (Theta) and gene flow (m), and their relation to differentiation (linearized F_{ST})

Model	AIC_C	Wi	Model coefficients				R^2_β	$R^2_{GLMM'm}$
			Theta	m	Resist	Geo		
Landscape: fragmented								
$F_{ST} \sim$ Theta	18.20	0.421	− 0.049 (− 0.0867, − 0.0130)	–	–	–	0.626	0.697
$F_{ST} \sim m$	18.52	0.359	–	− 0.010 (− 0.0228, − 0.0027)	–	–	0.048	0.035
$F_{ST} \sim$ Resist	20.71	0.120	–	–	− 0.004 (− 0.0082, 0.0011)	–	0.005	0.006
$F_{ST} \sim$ Geo	21.13	0.097	–	–	–	− 0.004 (− 0.0090, 0.0022)	0.004	0.005
Landscape: continuous								
$F_{ST} \sim$ Resist	− 15.45	0.973	–	–	0.003 (0.0023, 0.0030)	–	0.307	0.382
$F_{ST} \sim$ Geo	− 5.38	0.017	–	–	–	0.003 (− 0.0013, 0.0045)	0.292	0.362
$F_{ST} \sim$ Theta	− 3.06	0.005	− 0.001 (− 0.0043, 0.0028)	–	–	–	0.067	0.050
$F_{ST} \sim m$	− 2.85	0.005	–	0.00033 (− 0.0032, 0.0039)	–	–	0.009	0.013

Bracketed values under model coefficients are 95% confidence intervals. The Akaike information criterion corrected for small sample size (AIC_C), Akaike weights (Wi), and two variant R^2 statistics are listed for each model. Both R^2_β and $R^2_{GLMM'm}$ report the proportion of variation explained by the fixed effects included in the MLPE models

graphic distance explained less than one percent of the variation in pairwise F_{ST}. This result suggests that the patterns of genetic differentiation observed in the fragmented landscape are more related to genetic drift as opposed to the amount of gene flow. Within the continuous landscape, the resistance model received substantially more support than all of the remaining models evaluated ($AIC_C > 10$; Table 3). Moreover, resistance was the only predictor variable to exhibit a significant relationship with F_{ST}, suggesting that as resistance increases there is a significant increase in F_{ST} (Table 3). However, the R^2 statistics revealed that both resistance and geographic distance explained a similar proportion of variation in F_{ST} (resistance: $R^2_\beta = 0.307$; $R^2_{GLMM'm} = 0.382$; geographic distance: $R^2_\beta = 0.292$; $R^2_{GLMM'm} = 0.362$). Thus, the significant relationship observed between resistance and F_{ST} in the continuous landscape may reflect minor changes in resistance in an otherwise homogenous landscape that better predict F_{ST}. Finally, comparing the coefficients of predictor variables across landscapes revealed the greatest discrepancy to be among theta and m, where the coefficients for these two parameters were an order of magnitude greater in the fragmented landscape, while the coefficients for the landscape attributes were of similar scale.

Discussion

We analyzed eight polymorphic microsatellite loci to conduct a comparative genetic study of red-backed salamanders occupying landscapes with differing degrees of anthropogenic modification. Our results indicate the presence of genetic differentiation and population structuring in a fragmented urban landscape, whereas populations in a continuous forested landscape were undifferentiated. We found that in the fragmented landscape, spatial variation in theta best explained patterns of genetic differentiation, followed by gene flow, and the effect was an order of magnitude greater when compared to the continuous landscape. Conversely, resistance and geographic distance explained roughly an equivalent amount of variation in allele frequency differences among sites located in the continuous landscape. Overall, our results highlight the influence of gene flow and genetic drift in shaping patterns of genetic structure within a fragmented landscape at fine geographic scales.

Fragmented landscape

Most genetic dissimilarity in the fragmented landscape was exhibited by a single site (AR), while the remaining sites belonged to a single genetic cluster. The results of our MLPE models suggest that this pattern of population structure is best explained by variation in theta, a parameter closely tied to effective population size. There was also a significant relationship between pairwise F_{ST} and estimates of gene flow. Interpreting these model results together suggests that the marked differentiation of AR is induced by drift and that gene flow from the remaining sites is unable to mitigate the effects of genetic drift. The three sites that form a single genetic group in the fragmented landscape have larger values of theta and maintain higher levels of gene flow, and thus presumably have experienced weaker genetic drift. Recent work highlights that the contribution of genetic drift to the differentiation of red-backed salamander populations can vary across a moderate geographic scale (Hantak et al. 2019). This may explain why our results contrast with work conducted in other parts of the geographic range, which has documented pronounced genetic differentiation among fragmented sites despite populations being separated by similar geographic distances (0.6–4.1 km: Noël et al. 2007; current study: 1.9–8.4 km). We found that the resistance of the matrix surrounding the fragmented patches provided little ability to explain patterns of spatial genetic connectivity, which contradicts our initial prediction. However, the fact that extrinsic variables provided little predictive power in explaining variation in F_{ST} further suggests the presence of non-equilibrium processes in the fragmented landscape (Hutchison and Templeton 1999).

While the MLPE models provided strong evidence that the fundamental driver of genetic variation in the fragmented landscape is related to effective population size, multiple genetic diversity statistics seem to be in conflict with this conclusion. More specifically, while the AR site had the lowest estimate of theta and highest degree of relatedness based on F_{IS} values, this site also had the highest observed heterozygosity and allelic richness of all of the fragmented sites (Online Resource 2). Although this result is counterintuitive, the pattern of high genetic diversity coupled with low N_e has been observed in other salamander species inhabiting urban environments (e.g. *Salamandra salamandra*; Lourenço et al. 2017). Similar to *S. salamandra*, female red-backed salamanders can store spermatophores from multiple males (Sever 1997; Liebgold et al. 2006). Sperm storage can result in offspring with multiple paternity from a single clutch (Liebgold et al. 2006), suggesting a mechanism by which genetic diversity is retained in small populations (Lourenço et al. 2017). An alternative explanation for the patterns observed in the fragmented landscape, specifically the marked differentiation of AR, is the presence of unsampled subpopulations. Given the ability of red-backed salamanders to persist within small patches of microhabitat, it is possible that unsampled populations exist within the fragmented

landscape we surveyed. Therefore, AR may have been colonized by individuals belonging to a subpopulation that is differentiated from the deme that DB, LV, and EC belong to, and the lack of gene flow in and out of AR would act to magnify preexisting differences especially when N_e is small (see Gibbs 1998b for additional discussion).

Continuous landscape

The results of the MLPE models revealed a significant positive relationship between resistance and variation in F_{ST} values. However, in comparing the marginal R^2 statistics, resistance and geographic distance explain roughly equivalent amounts of variation in allele frequencies among sites. This is not surprising given the strong correlation between the two variables (Mantel $r = 0.97$). Overall, this suggests that gene flow in the continuous landscape is limited by distance, but that resistance was able capture minor changes in homogeneity that slightly better predict variation in pairwise F_{ST} compared to geographic distance. Our results are similar to Noël et al. (2007; Quebec) in that we observed no differentiation among sites and failed to detect genetic structuring across a variety of statistical approaches. These results contrast with the differentiation observed by Cabe et al. (2007), where populations within continuous habitat located in Virginia exhibited weak, but detectable, differentiation at a fine scale (≤ 2 km). The similarity of our continuous landscape to that of Noël et al. (2007) is likely attributable to both studies being conducted in formerly glaciated range portions where patterns of differentiation tend to be less pronounced relative to unglaciated regions (Highton and Webster 1976; Jordan et al. 2009; Cameron et al. 2017).

Landscape comparison

The model coefficients for landscape resistance revealed effects of similar magnitude in both landscapes. However, comparing the mean resistance among the least differentiated sites (DB, LV, and EC) to the mean resistance of the continuous landscape revealed a much higher cost of movement in the fragmented landscape (DB, LV, EC = 0.94; continuous = 0.53). Comparisons of locus-specific estimates of G''_{ST}, excluding the most differentiated site within the fragmented landscape (AR), revealed no statistical difference in the amount of genetic differentiation between landscapes despite a higher cost of movement. It is important to note that resistance surfaces were derived from estimates of habitat suitability, suggesting that the presence of low suitability habitat between fragmented patches does not completely impede gene flow. Red-backed salamanders possess several ecological traits that may enable them to utilize marginal habitats within suburban landscapes. For example, red-backed salamanders exhibit much less sensitivity to habitat perturbation compared to other forest dwelling salamander species (e.g. *Ambystoma maculatum*, *Notophthalmus viridescens*; Gibbs 1998c) and have been documented at high densities in disturbed habitat (Anthony and Pfingsten 2013 and citations within). Red-backed salamanders living in these habitats are able to use non-native, and in some cases invasive, prey (Maerz et al. 2005; Walton et al. 2006). Recent evidence indicates that marginal habitats (edge/meadow) can support population sizes comparable to woodland habitat, with no significant difference in physical condition of individuals residing in edge/meadow habitats compared to woodland (Riedel et al. 2012). Although the long-term persistence of populations occupying degraded or marginal habitats is unknown, the high densities at which red-backed salamanders can occur in these habitats potentially offsets the high mortality rate associated with dispersal in landscapes with reduced permeability (Gibbs 1998b). Despite suburban areas having a high road density, there is evidence to suggest that roads typical of residential areas would not pose strong genetic barriers to red-backed salamanders (Marsh et al. 2008), especially when dispersal across roads is most likely to occur at night. Finally, red-backed salamanders have been documented dispersing through open fields, suggesting that dispersal may not be limited by a lack of canopy cover (Marsh et al. 2004).

Conservation implications

Habitat loss and modification remain the leading drivers of the global decline of amphibians, yet there is considerable variation in the sensitivity to this threat across taxonomic groups (Nowakowski et al. 2017). A major source of the variation in the sensitivity to habitat fragmentation is related to the ecological traits that influence a species' ability to tolerate and occupy matrix habitat, which can govern the strength of the fragmentation effects (Ewers and Didham 2006; Nowakowski et al. 2017). Documenting cases where fragmentation does not have the expected, negative result is critical to forming a more general understanding of the traits that contribute to variation in sensitivity to habitat fragmentation. Our results suggest that red-backed salamanders can utilize marginal habitat within a highly modified landscape to maintain a degree of connectivity comparable to a large forested tract of habitat. This implies that the effects of fragmentation may be negligible for this species. Red-backed salamanders are a robust, generalist species and as a result, the negative genetic consequences of habitat modification may only manifest in the most extreme cases. Additionally, given the extent of this species' distribution, the effects of habitat modification may vary geographically, and depend on population history within an area. As such, careful consideration should be taken when using red-backed salamanders as an ecological indicator species of forest ecosystem change.

Compliance with ethical standards

Conflict of interest The authors declare that they have no conflict of interests.

References

Alford RA, Richards SJ (1999) Global amphibian declines: a problem in applied ecology. Annu Rev Ecol Evol Syst 1:133–165

Almedia-Gomes M, Rocha CFD (2014) Landscape connectivity may explain anuran species distribution in an Atlantic forest fragmented area. Landsc Ecol 29:29–40

Anthony CD, Pfingsten RA (2013) Eastern red-backed Salamander, *Plethodon cinereus*. In: Pfingsten RA, Davis JG, Matson TO, Lipps G, Wynn D, Armitage BJ (eds) Amphibians of Ohio. Ohio Biological Survey Bulletin new series, vol 17. Ohio Biological Survey, Ohio, pp 335–360

Barr KR, Kus BE, Preston KL, Howell S, Perkins E, Vandergast AG (2015) Habitat fragmentation in coastal southern California disrupts genetic connectivity in the cactus wren (*Campylorhynchus brunneicapillus*). Mol Ecol 24:102349–102363

Bartoń K (2013) MuMIn: multi-model inference. R package version 1.9.13. https://CRAN.R-project.org/package=MuMIn

Bates D, Mächler M, Bolker B, Walker S (2015) Fitting linear mixed-effects models using lme4. J Stat Softw 67:1–48

Beerli P (2008) Migrate version 3.0: a maximum likelihood and Bayesian estimator of gene flow using the coalescent. http://popgenscs.edu/migrate.html. Accessed 01 Jun 2016

Beerli P (2009) How to use MIGRATE or why are Markov chain Monte Carlo programs difficult to use? In: Bertorelle G, Bruford M, Hauffe H, Rizzoli A, Vernesi C (eds) Population genetics for animal conservation. Cambridge University Press, Cambridge, pp 39–77

Bowne DR, Bowers MA (2004) Interpatch movements in spatially structured populations: a literature review. Ecol 19:1–20

Breiman L (2001) Random forests. Mach Learn 45:5–32

Cabe PR, Page RB, Hanlon TJ, Aldrich ME, Connors L, Marsh DM (2007) Fine- scale population differentiation and gene flow in a terrestrial salamander (*Plethodon cinereus*) living in continuous habitat. Heredity 98:53–60

Cameron AC, Anderson JJ, Page RB (2017) Assessment of intra and interregional genetic variation in the Eastern Red-backed Salamander, *Plethodon cinereus*, via analysis of novel microsatellite markers. PLoS ONE 12:e0186866

Clarke RT, Rothery P, Raybould AF (2002) Confidence limits for regression relationships between distance matrices: estimating gene flow with distance. J Agric Biol Environ Stat 7:361

Converse PE, Kuchta SR, Roosenburg WM, Henry PF, Haramis GM, King TL (2015) Spatiotemporal analysis of gene flow in Chesapeake Bay Diamondback Terrapins (*Malaclemys terrapin*). Mol Ecol 24:5864–5876

Cook RD (1977) Detection of influential observation in linear regression. Technometrics 19:15–18

Cushman SA, McRae BH, McGarigal K (2016) Basics of landscape ecology: an introduction to landscapes and population processes for landscape geneticists. In: Balkenhol N, Cushman SA, Storfer AT, Waits LP (eds) Landscape genetics: concepts, methods applications. Wiley Blackwell, UK, pp 11–30

Davic RD, Welsh HH Jr (2004) On the ecological roles of salamanders. Annu Rev Ecol Evol Syst 35:405–434

Do C, Waples RS, Peel D, Macbeth GM, Tillett BJ, Ovenden JR (2014) NeEstimator v2: re-implementation of software for the estimation of contemporary effective population size (Ne) from genetic data. Mol Ecol Resour 14:209–214

Dray S, Dufour AB (2007) The ade4 package: implementing the duality diagram for ecologists. J Stat Softw 22:1–20

Duellman WE, Trueb L (1986) Biology of amphibians. JHU Press, Baltimore

Earl DA, vonHoldt BM (2012) STRUCTURE HARVESTER: a website and program for visualizing STRUCTURE output and implementing the Evanno method. Conserv Genet Resour 4:359–361

Edwards LJ, Muller KE, Wolfinger RD, Qaqish BF, Schabenberger O (2008) An R2 statistic for fixed effects in the linear mixed model. Stat Med 27:6137–6157

Evanno G, Regnaut S, Goudet J (2005) Detecting the number of clusters of individuals using the software STRUCTURE: a simulation study. Mol Ecol 14:2611–2620

Ewers RM, Didham RK (2006) Confounding factors in the detection of species responses to habitat fragmentation. Biol Rev 81:117–142

Excoffier L, Smouse PE, Quattro JM (1992) Analysis of molecular variance from metric distances among DNA haplotypes: application to human mitochondrial DNA restriction data. Genetics 131:479–491

Fenderson LE, Kovach AI, Litvaitis JA, O'Brien KM, Boland KM, Jakubas WJ (2014) A multiscale analysis of gene flow for the New England cottontail, an imperiled habitat specialist in a fragmented landscape. Ecol Evo 4:1853–1875

Fisher-Reid MC, Engstrom TN, Kuczynski CA, Stephens PR, Wiens JJ (2013) Parapatric divergence of sympatric morphs in a salamander: incipient speciation on Long Island? Mol Ecol 22:4681–4694

Friedman JH (2002) Stochastic gradient boosting. Comput Stat Data Anal 38:367–378

Garza JC, Williamson EG (2001) Detection of reduction in population size using data from microsatellite loci. Mol Ecol 10:305–318

Gibbs JP (1998a) Amphibian movements in response to forest edges, roads, and streambeds in southern New England. J Wildl Manage 62:584–589

Gibbs JP (1998b) Genetic structure of redback salamander *Plethodon cinereus* populations in continuous and fragmented forests. Biol Conserv 86:77–81

Gibbs JP (1998c) Distribution of woodland amphibians along a forest fragmentation gradient. Landsc Ecol 13:263–268

Grant AH, Liebgold EB (2017) Color-biased dispersal inferred by Fine-Scale genetic spatial autocorrelation in a color polymorphic salamander. J Hered 108:588–593

Hansen MC, Potapov PV, Moore R, Hancher M, Turubanova SA, Tyukavina A et al (2013) High-resolution global maps of 21st-century forest cover change. Science 342:850–853

Hanski I (1998) Metapopulation dynamics. Nature 396:41–49

Hantak MM, Page RB, Converse PE, Anthony CD, Hickerson CAM, Kuchta SR (2019) Do genetic structure and landscape heterogeneity impact color morph frequency in a polymorphic salamander? Ecography 42:1–12

Highton R, Webster TP (1976) Geographic protein variation and divergence in populations of the salamander *Plethodon cinereus*. Evolution 30:33–45

Hillman SS, Drewes RC, Hedrick MS, Hancock TV (2014) Physiological vagility and its relationship to dispersal and neutral genetic heterogeneity in vertebrates. J Exp Biol 217:3356–3364

Holm S (1979) A simple sequentially rejective multiple test procedure. Scand J Stat 6:65–70

Homer CG, Dewitz JA, Yang L, Jin S, Danielson P, Xian G et al (2015) Completion of the 2011 National Land Cover Database for the conterminous United States-representing a decade of land cover change information. Photogramm Eng Remote Sens 81:345–354

Hutchison DW, Templeton AR (1999) Correlation of pairwise genetic and geographic distance measures: inferring the relative influences of gene flow and drift on the distribution of genetic variability. Evolution 53:1898–1914

Jaeger B (2016) R2glmm: computes R squared for mixed (multilevel) models. *R package version 0.1, 1*

Jaeger RG, Forester DC (1993) Social behavior of plethodontid salamanders. Herpetologica 49:163–175

Jaeger RG, Gollmann B, Anthony CD, Gabor CR, Kohn NR (2016) Behavioral ecology of the eastern red-backed salamander: 50 years of research. Oxford University Press, Oxford

Jakobsson M, Rosenberg NA (2007) CLUMPP: a cluster matching and permutation program for dealing with label switching and multimodality in analysis of population structure. Bioinformatics 23:1801–1806

Jombart T, Collins C (2015) A tutorial for discriminant analysis of principal components (DAPC) using adegenet 2.0. 0. Imp Coll London-MRC Cent Outbreak Anal Model 43

Jombart T, Devillard S, Balloux F (2010) Discriminant analysis of principal components: a new method for the analysis of genetically structured populations. BMC Genet 11:94

Jordan MA, Morris DA, Gibson SE (2009) The influence of historical landscape change on genetic variation and population stricture of a terrestrial salamander (*Plethodon cinereus*). Conserv Genet 10:1647–1658

Liebgold EB, Cabe PR, Jaeger RG, Leberg PL (2006) Multiple paternity in a salamander with socially monogamous behaviour. Mol Ecol 15:4153–4160

Liebgold EB, Brodie ED III, Cabe PR (2011) Female philopatry and male-biased dispersal in a direct developing salamander, *Plethodon cinereus*. Mol Ecol 20:249–257

Lourenço A, Álvarez D, Wang IJ, Velo-Antón G (2017) Trapped within the city: integrating demography, time since isolation and population-specific traits to assess the genetic effects of urbanization. Mol Ecol 26:1498–1514

Maerz JC, Karuzas JM, Madison DM, Blossey B (2005) Introduced invertebrates are important prey for a generalist predator. Divers Distrib 11:83–90

Mantel N (1967) The detection of disease clustering and a generalized regression approach. Cancer Res 27:209–220

Marsh DM, Trenham PC (2001) Metapopulation dynamics and amphibian conservation. Conserv Biol 15:40–49

Marsh DM, Thakur KA, Bulka KC, Clarke LB (2004) Dispersal and colonization through open fields by a terrestrial, woodland salamander. Ecology 85:3396–3405

Marsh DM, Page RB, Hanlon TJ, Bareke H, Corritone R, Jetter N et al (2007) Ecological and genetic evidence that low-order streams inhibit dispersal by red-backed salamanders (*Plethodon cinereus*). Can J Zool 85:319–327

Marsh DM, Page RB, Hanlon TJ, Corritone R, Little EC, Seifert DE, Cabe PR (2008) Effects of roads on patterns of genetic differentiation in red-backed salamanders, *Plethodon cinereus*. Conserv Genet 9:603–613

Mathis A, Jaeger RG, Keen WH, Ducey PK, Walls SG, Buchanan BW (1995) Aggression and territoriality by salamanders and a comparison with the territorial behavior of frogs. In: Heatwole H, Sullivan BK (eds) Amphibian biology volume 2: social behaviour surrey beatty and sons. Chipping Norton, New South Wales, pp 633–676

McRae BH, Dickson BG, Keitt TH, Shah VB (2008) Using circuit theory to model connectivity in ecology, evolution, and conservation. Ecology 89:2712–2724

Meirmans PG (2015) Seven common mistakes in population genetics and how to avoid them. Mol Ecol 24:3223–3231

Meirmans PG, Hendrick PW (2011) Assessing population structure: F_{ST} and related measures. Mol Ecol Resour 11:5–18

Nakagawa S, Schielzeth H (2013) A general and simple method for obtaining R2 from generalized linear mixed-effects models. Methods Ecol Evol 4:133–142

Nei M, Chesser RK (1983) Estimation of fixation indices and gene diversities. Ann Hum Genet 47:253–259

Noël S, Lapointe FJ (2010) Urban conservation genetics: study of a terrestrial salamander in the city. Biol Conserv 143:2823–2831

Noël S, Ouellet M, Galois P, Lapointe FJ (2007) Impact of urban fragmentation on the genetic structure of the eastern red-backed salamander. Conserv Genet 8:599–606

Nowakowski AJ, Thompson ME, Donnelly MA, Todd BD (2017) Amphibian sensitivity to habitat modification is associated with population trends and species traits. Glob Ecol Biogeogr 26:700–712

Paquette SR (2012) PopGenKit: useful functions for (batch) file conversion and data resampling in microsatellite datasets. R Package Version, 1

Peakall ROD, Smouse PE (2012) GENALEX 6.5: genetic analysis in excel. Population genetic software for teaching and research—an update. Bioinformatics 28:2537–2539

Peterman WE (2018) ResistanceGA: an R package for the optimization of resistance surfaces using genetic algorithms. Methods Ecol Evol 9:1638–1647

Piry S, Luikart G, Cornuet JM (1999) BOTTLENECK: a program for detecting recent effective population size reductions from allele data frequencies. J Hered 90:502–503

Pritchard JK, Stephens M, Donnelly P (2000) Inference of population structure using multilocus genotype data. Genetics 155:945–959

Reiter MK, Anthony CD, Hickerson CAM (2014) Territorial behavior and ecological divergence in a polymorphic salamander. Copeia 3:481–488

Riedel BL, Russell KR, Ford WM (2012) Physical condition, sex, and age-class of eastern red-backed salamanders (*Plethodon cinereus*) in forested and open habitats of West Virginia, USA. Int J Zool 2012:623730

Rousset F (2008) genepop'007: a complete re-implementation of the genepop software for Windows and Linux. Mol Ecol Resour 8:103–106

Samarasin P, Shuter BJ, Wright SI, Rodd FH (2017) The problem of estimating recent genetic connectivity in a changing world. Conserv Biol 31:126–135

Schuelke M (2000) An economic method for the fluorescent labeling of PCR fragments. Nat Biotechnol 18:233–234

Semlitsch RD (2008) Differentiating migration and dispersal processes for pond-breeding amphibians. J Wildl Manage 72:260–267

Sever DM (1997) Sperm storage in the spermatheca of the red-back salamander, *Plethodon cinereus* (Amphibia: Plethodontidae). J Morphol 234:131–146

Slatkin M (1995) A measure of population subdivision based on microsatellite allele frequencies. Genetics 139:457–462

Spear SF, Balkenhol N, Fortin MJ, McRae BH, Scribner KIM (2010) Use of resistance surfaces for landscape genetic studies: considerations for parameterization and analysis. Mol Ecol 19:3576–3591

R Core Team (2016) R: A language and environment for statistical computing. R Foundation for Statistical Computing, Vienna, Austria. https://www.R-project.org/

Templeton AR, Robertson RJ, Brisson J, Strasburg J (2001) Disrupting evolutionary processes: the effect of habitat fragmentation on

collared lizards in the Missouri Ozarks. Proc Natl Acad Sci USA 98:5426–5432

Thuiller W, Lafourcade B, Engler R, Araújo MB (2009) BIOMOD—a platform for ensemble forecasting of species distributions. Ecography 32:369–373

Van Oosterhout C, Hutchinson WF, Wills DP, Shipley P (2004) MICRO-CHECKER: software for identifying and correcting genotyping errors in microsatellite data. Mol Ecol Notes 4:535–538

Vandergast AG, Bohonak AJ, Weissman DB, Fisher RN (2007) Understanding the genetic effects of recent habitat fragmentation in the context of evolutionary history: phylogeography and landscape genetics of a southern California endemic Jerusalem cricket (Orthoptera: Stenopelmatidae: *Stenopelmatus*). Mol Ecol 16:977–992

Walton BM, Tsatiris D, Rivera-Sostre M (2006) Salamanders in forest-floor food webs: invertebrate species composition influences top–down effects. Pedobiologia 50:313–321

Waples RS, Do CHI (2008) LDNE: a program for estimating effective population size from data on linkage disequilibrium. Mol Ecol Res 8:753–756

Watling JI, Braga L (2015) Desiccation resistance explains amphibian distributions in a fragmented tropical forest landscape. Landsc Ecol 30:1449–1459

Weir BS, Cockerham CC (1984) Estimating F-statistics for the analysis of population structure. Evolution 38:1358–1370

Welsh HH, Droege S (2001) A case for using plethodontid salamanders for monitoring biodiversity and ecosystem integrity of North American forests. Con Bio 15:558–569

Yue GH, David L, Orban L (2007) Mutation rate and pattern of microsatellites in common carp (*Cyprinus carpio* L.). Genetica 129:329–331

Zhdanova OL, Pudovkin AI (2008) Nb_HetEx: a program to estimate the effective number of breeders. J Hered 99:694–695